Supporting Information

Rohde *et al.* 10.1073/pnas.0803763105

SI Materials and Methods

Fluorimeter. To measure concentrations of microorganisms independent of taxa we used a Photon Systems TUCS (Targeted UV Chemical Sensor) fluorimeter with six phototubes (Hamamatsu H5773P-01) arranged around a 224-nm laser and covered with five bandpass filters at 300 ± 10, 320 ± 10, 340 ± 10, 360 ± 10, and 380 ± 10 nm, and a long-pass filter for wavelengths ≥420 nm. The laser excites fluorescence of protein-bound Trp, which is present in all cells, in a cylindrical region of ice ≈0.5 cm deep with diameter ≈200 μm at 300-μm distance intervals. Fig. S1 shows fluorescence data that illustrate how the TUCS distinguishes microbes from mineral grains. The region at depth 2954 m in the Greenland GISP2 ice had ≈4 ppmV methane (1), an order of magnitude higher than values at depths just a few decimeters above and below that depth (unpublished measurements by Todd Sowers), and were shown by direct cell counts (2) to have an order of magnitude higher concentration of all cells and of methanogens than the normal values. Spectra with shapes consistent with protein-bound Trp (correlation factor $R \geq 0.75$) were represented by red points in Fig. 1 *Upper* and in Fig. S1. Those with different shapes ($R < 0.75$), referred to as non-Trp in the text, were represented by blue points in the same figures.

Scanning Fluorimetry. 17,000 m of ice cores are stored in the dark at NICL at −36°C. We were allotted 80 h in spring 2006 and 80 h in spring 2007 to map fluorescence of ice cores. Our protocol was to remove a batch of cores from the repository at −36°C for preparation and scanning in an adjacent laboratory at −25°C and at the end of each day to return them to the repository so as to minimize sublimation of ice. We chose portions of 13.2-cm-diameter ice cores that had been cut lengthwise on a band saw to a thickness of ≈7 cm and polished on the flat side. We scraped the flat side of each core with a microtome blade to remove ≈1 mm of ice and leveled the core on a stage that could be translated up to 1.2 m at a speed of ≈3 mm s^{-1}. The main reason for scanning the flat surface is so that the volume from which laser-induced fluorescence is accepted by the photon counters is far from the original outer surface of the ice core. We considered this to be necessary in view of the fact that measurements of the radial distribution of microbes in the GISP2 ice core usually showed a high level of contamination in the outer few mm, whereas within ≈4 cm of the center the microbial concentration was independent of radius (2).

To take data, a fluorimeter was mounted on a jack above the core and adjusted in lateral position and in height so that the exit point of the laser beam was ≈1 mm above the surface of the ice. In April 2006 we studied samples from Vostok Station, Siple Dome, and Taylor Dome, Antarctica, and from various depths in a 3053-m GISP2 core. In March 2007 we studied additional sections from GISP2 as well as sections from a West Antarctic Ice Sheet (WAIS) Divide 295-m core.

In 4 weeks of scanning, we acquired spectra of protein-bound Trp on 130 sections of ice cores. The data comprised ≈240,000 spectra. After we discovered that almost every Vostok core section was contaminated with an organic background, probably due to leakage of drilling fluid into microcracks in the ice, we decided to concentrate on GISP2 ice (66% of the core sections) and on WAIS Divide ice (17% of the core sections), neither of which showed evidence of contamination. Results from the WAIS Divide study will be published at a future date.

Preparation of Ice Samples for Extraction and Treatment of Microbial Cells. We sterilized our glassware by baking at 600°C up to 5 h. In a sterile laminar flow hood, we removed >30% of the exterior of each GISP2 ice sample by rinsing it sequentially with 10 M HCl, DNase- and RNase-free sterile water, 10 M NaOH, and a final rinse in sterile water to eliminate any contamination that might have been introduced during the drilling process or subsequent handling of the samples. This treatment was designed to remove and destroy not only cells but also bacterial spores and nucleic acid from the sample exterior. To test our methods, we made numerous ice samples, coated them with various types of bacteria including *E. coli* and *M. luteus*, and with *B. subtilis* spores, at concentrations of $\geq 10^8$ cells ml^{-1}, subjected them to the same sterilizing procedure we used with the GISP2 sample, and verified, with direct counting methods and culturing, that none of the cells and spores coated on the ice surfaces made it into the final test sample. We processed the GISP2 ice samples together with control samples in a double-blind manner.

Enumeration of Syto-23-Stained Cells and of Methanogens. For our ground-truth studies of cell concentration, we melted 4–7 ml of an interior ice sample at each depth of interest, immediately stained the cells in the melted ice with up to 20 μM Syto-23, and filtered a known volume of the melted ice through a circular region ≈1 cm in diameter on a Nuclepore polycarbonate filter with 0.015 μm pore size. We used a Zeiss Axiovert epifluorescence microscope with a 100× objective at room temperature to count all of the fluorescing cells on the region of the filter through which the solution had passed. For Syto-23-stained cells, the volume in which cells were counted was chosen to achieve a statistical error <3%.

Using the same microscope, we counted unstained cells from the sample interior by viewing their F420 autofluorescence. To examine the cells without introducing chemical artifacts, we omitted a fixation process. Using excitation at 420 nm and a long-pass filter at 460 nm, we detected this fluorescence in a small fraction of cells in the band ≈460–490 nm. We were able to account for possible interference due to autofluorescence of μm-size mineral grains that might accompany the microbes by taking advantage of the narrow excitation spectrum of F420 and its relatively high photobleaching rate in the concentrated beam of the epifluorescence microscope. By photobleaching our samples after counting cells and then counting those cells with multiple excitation/emission wavelengths, we were able to subtract the mineral background. We tested these methods using *M. jannaschii* and mineral grains filtered from melted GISP2 ice. The results showed that mineral grains from GISP2 were far more resistant to photobleaching than were methanogens. Moreover, the minerals tended to fluoresce over a broad spectrum of excitation wavelengths, whereas F420 fluoresced only at ≈420 nm excitation. With exposure to oxygen, the F420 degrades during the course of a day or so and loses its fluorescence, so that observations were made within ≈1 h after exposure.

Although F420 has been detected in cells of several members of all three domains (3), it is abundant only in methanogens. In nonmethanogens its concentration is typically lower by several orders of magnitude (4), and its detection requires purification.

Calibrations of the Fluorimeter with Direct Counts of Microbes in GISP2 Ice Cores. To check whether methane spikes found at 2954, 3018, and 3036 m in GISP2 ice (1) were due to *in situ* microbial metabolism and to find out how sharply the microbial concen-

trations were peaked in depth (2), we studied samples from just above, just below, and at those depths. We also obtained ice samples at seven random depths from 500 to 3,000 m as controls. We found not only that the microbial concentrations inferred from both the TUCS and F420 epifluorescence microscopy were peaked at 2,954, 3,018, and 3,036 m to within 0.1 to 0.2 m, but that two of the seven randomly chosen depths (2,238 and 3,000 m) also had large cell concentrations (2). Methane had not been measured within 2 m of those depths (1, 5).

To relate cell concentration to fluorescence intensity we mapped the profiles of protein-bound Trp fluorescence at 2,238, 2,954, 3,018, 3,036, and 3,000 m. Comparison of the fluorescence results and the cell counts (2) led to the following conversion factors:

$$C_{\text{cells}} = 1.52 \times 10^6 \text{cm}^{-3} \times \langle I_{\text{Trp}} \rangle, \qquad \textbf{[S1]}$$

where $C_{\text{cells}}(\text{cm}^{-3})$ is cell concentration and the brackets signify the fluorescence intensity averaged over a region corresponding to the 6-ml volume of ice melted and filtered for direct counts (1). This calibration is valid for cells with the same average dry weight, 48 fg, that were measured in ref. 1.

To relate the number of cells in an illuminated volume to fluorimeter intensity at that depth requires an estimate of the volume within which they are distributed. The volume within which a fluorimeter excites fluorescence is $\pi r_{\text{beam}}^2 \Delta z$. For the TUCS, with $r_{\text{beam}} \approx 100$ μm and $\Delta z \approx 0.5$ cm, $V_{\text{TUCS}} = 1.57 \times 10^{-4}$ cm^3. If the cells fill a volume $V \leq V_{\text{TUCS}}$, the number of cells in that volume element is

$$N_{\text{cells}} = 243 \times \langle I_{\text{Trp}} \rangle \qquad \textbf{[S2]}$$

For typical intensities $\langle I_{\text{Trp}} \rangle = 0.02$ to 1.5 units, C_{cells} ranges from 3.5×10^4 to 2.6×10^6 cm^{-3} and N_{cells} ranges from $\approx$6 to 420 cells in 1.57×10^{-4} cm^3. Background levels encountered in our scans of ice cores range from $\approx$0.002 to 0.005 unit, corresponding to 0.55 to 1.4 cells.

1. Brook EJ, Sowers T, Orchardo J (1996) Rapid variations in atmospheric methane concentration during the past 110,000 years. *Science* 273:1087–1091.
2. Tung HC, Bramall NE, Price PB (2005) Microbial origin of excess methane in glacial ice and implications for life on Mars. *Proc Natl Acad Sci USA* 102:18292–18296.
3. Purwantini E, Daniels L (1998) Molecular analysis of the gene encoding F420-dependent glucose-6-phosphate dehydogenase from *Mycobacterium smegmatis*. *J Bacteriol* 180:2212–2219.
4. Lin XL, White RH (1986) Occurrence of coenzyme F_{420} and and its γ-monoglutamyl derivative in non-methanogenic archaebacteria. *J Bacteriol* 168:444–448.
5. Chappellaz J, Brook E, Blunier T, Malaizé B (1997) CH_4 and $d^{18}O$ of O_2 records from Antarctic and Greenland ice: A clue for stratigraphic disturbance in the bottom part of the Greenland Ice Core Project and the Greenland Ice Sheet Project 2 ice cores. *J Geophys Res* 102:26547–26557.
6. Tung HC, Price PB, Bramall NE, Vrdoljak G (2006) Microorganisms metabolizing on clay grains in 3-km-deep Greenland basal ice. *Astrobiology* 6:69–86.

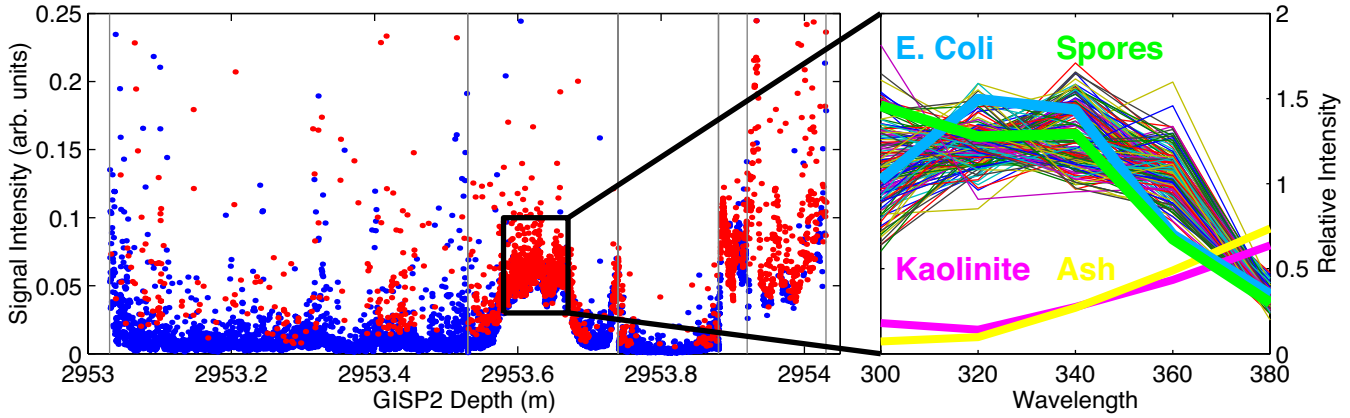

Fig. S1. (*Left*) Intensity of fluorescence in the TUCS along a 1-m section of GISP2. Points in red have a spectral shape consistent with fluorescence of protein-bound Trp with maximum amplitude at 320 to 340 nm; points in blue have spectra with different shape that are due to organic aerosols and mineral grains. (*Right*) Spectra for all measurements in the boxed region compared with spectra for lab specimens for bacteria and minerals. Blue and green curves are for *E. coli* and spores, respectively; yellow and pink curves are for volcanic ash and kaolinite grains scaled up by a factor 100 for visibility.

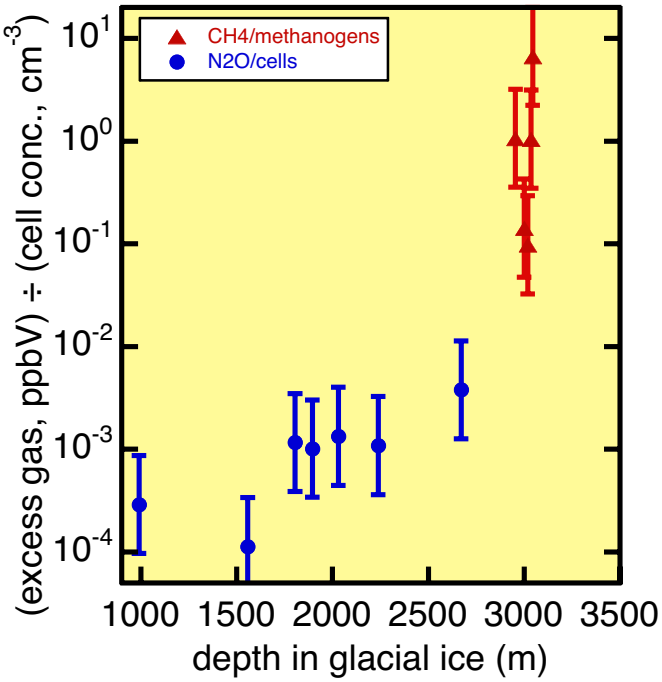

Fig. S2. Ratio of excess gas (ppbV) to excess microbial concentration (cm^{-3}) versus depth in GISP2 ice core, obtained from data at depths indicated in ref. 6 and Fig. 2.